Predicted versus Actual Performance of the Model Scale Compulsator System

J. R. Kitzmiller, K. G. Cook, J. J. Hahne, T. J. Hotz, S. M. Manifold, J. A. Pappas, C. E. Penney, S. B. Pratap, B. Rech, R. F. Thelen, W. A. Walls, M. D. Werst, R. C. Zowarka, W. W. Rienstra, and A. Nejezchleb

***Abstract*—Performance testing of the model-scale CPA was recently completed at the University of Texas Center for Electromechanics. A major part of the project was the development of design and simulation codes that would accurately represent the performance of pulsed alternators. This paper discusses the components of the system and its operational sequence. Details of the performance simulation model are presented along with test data. The test result is compared to the predicted data.**

I. Introduction

As a power source for electric guns, pulsed alternators (or compulsators, referred to as CPA) have been under development for many years [1]–[6], with a wide range of configurations including: rotating armature, rotating field, iron-core, air-core, externally excited, and self-excited.

The transition from iron-core to air-core identified the need for self-excitement in the system, and has made the CPA more adaptable to future design of fieldable electric gun platforms. This paper describes a model scale CPA system recently developed and tested at the University of Texas Center for Electromechanics (UT-CEM). The model scale CPA is the first air-core CPA tested to its full design capability. This development program also proved that the design and performance codes can accurately predict the behavior of CPA. This paper compares design predictions to actual performance.

II. System Description and Operation

Fig. 1 shows the essential hardware components of the CPA. Four subsystems make up the CPA-railgun system (or pulse-power system): the compulsator, switches, controls, and load. Fig. 2 shows the secondary hardware items essential for the testing of a CPA system. Energy required for the railgun launch is derived from the electromechanical conversion of power (at the GW level) from the CPA rotor. A rectifier converts the AC power to DC power. Although controlled switch devices are preferred for optimal control and efficiency of the CPA-based system, resource limitations required the use of a diode-based rectifier for field charging and main load or railgun discharging.

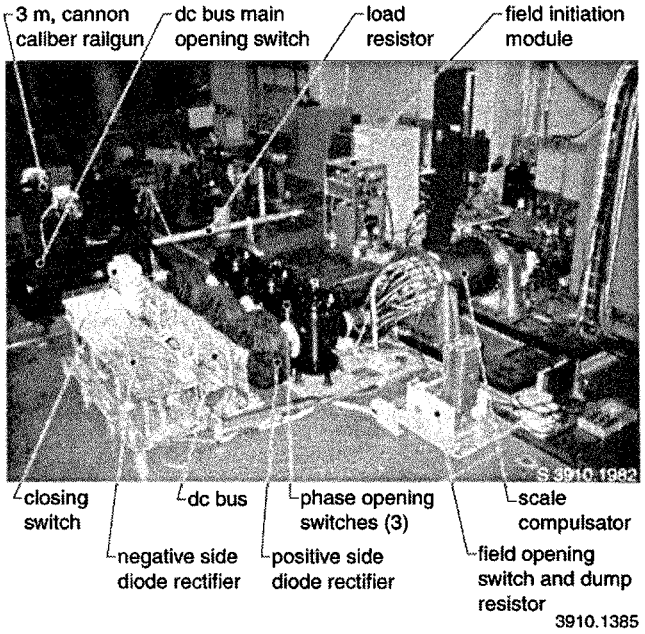

Fig. 1. Scale compulsator test site at UT-CEM.

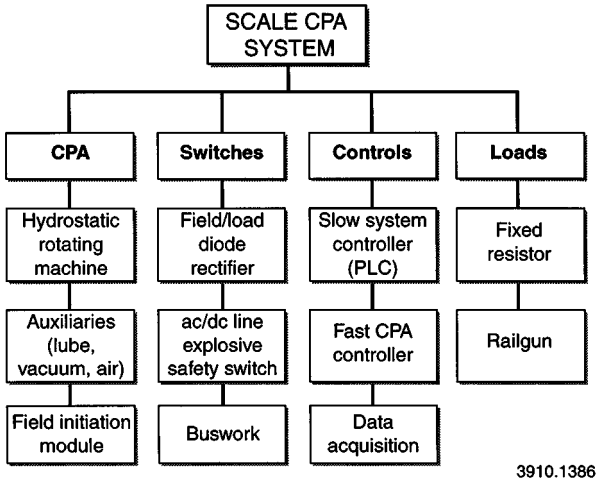

Fig. 2. Scale compulsator system component tree.

However, when diodes are used, field self-excitation cannot be stopped by simple command to the rectifier. Self-excitation can only be halted, once begun, by depleting the intertial energy store of the CPA, or by physically interrupting the electrical buses feeding the coil and load.

Since damage may occur to the electrical windings through overheating when the energy store is depleted, the system was

Manuscript received December 21, 1999. This project was supported by the U.S. Army under Contract DAAA21-92-C-0105. The COTR was Dr. E. Schmidt.

J. R. Kitzmiller, K. G. Cook, J. J. Hahne, T. J. Hotz, S. M. Manifold, J. A. Pappas, C. E. Penney, S. B. Pratap, B. Rech, R. F. Thelen, W. A. Walls, M. D. Werst, and R. C. Zowarka are with The University of Texas at Austin Center for Electromechanics.

W. W. Rienstra and A. Nejezchleb are with the Science Applications International Corporation.

Publisher Item Identifier S 0018-9464(01)00162-5.

equipped with several ac and dc bus explosive opening switches to control the current flow during a discharge sequence. The entire CPA discharge sequence lasts less than 0.1 s, and is controlled almost entirely through timers and explosive firing boxes. The sequence of a CPA test is described below.

- The rotor is brought up to its test speed using a controlled hydrostatic transmission system and high-speed gearbox. This controller is typically a programmable logic controller (PLC) referred to as the slow controller.
- Once the rotor is confirmed at speed and the PLC has verified all subsystems are operating correctly, the slow controller actuates the rotor brushes and then the discharge sequence is handed over to the CPA firing and fault control module (FFCM).
- The FFCM first triggers the field initiation module SCR's, which discharge a pair of precharged 25 kJ capacitors via the compulsator brushes and into the spinning field coil on the rotor. This small "seed current" creates magnetic flux and a small voltage is generated within the generator armature windings.
- Since the armature windings are connected back to the field winding via a full wave diode rectifier, voltage and current begin to build within the generator exponentially, drawing upon the rotor mechanical energy as the prime energy source for this process.
- After an extremely short period, the field current and armature voltage have reached their predetermined set points and the main discharge sequence commences.
- Because half of the field rectification bridge is also used to deliver current to the main generator load, an additional explosive closing switch is located on the dc bus between the diode bridge and railgun or load. Following a precise charging time interval, the FFCM activates the explosive closing switch at an armature phase firing angle (interval and angle preprogrammed) to initiate commutation of the current into the load.
- Naturally commutated currents flow to the railgun (or fixed load) as the generator turns through each armature phase. When the appropriate number of current cycles has been delivered, each ac armature phase is interrupted near natural current zeros at timed intervals using the phase opening switches (Fig. 1). Switch timing is determined from the performance code.
- The last phase is interrupted along with another auxiliary dc opening switch that safely ensures the railgun is disconnected from the CPA. Finally, the field dc explosive opening switch is actuated, forcing the field current to decay through a passive resistor bank (Fig. 1).
- The motoring controller brakes the rotor using the hydrostatic transmission, and data is collected and analyzed.

III. Modeling and Analysis

The need for an accurate performance model for rail gun systems was recognized early in the electric gun program [7], [8]. Quite a bit of effort was expended to understand the rail gun and armature interactions and their effects on projectile performance [9]–[11]. In addition, some attention was paid to mechanical opening and closing switches [12], [13]. However, the pulsed power supplies in these early systems were largely static capacitor banks or inductor arrays. These arrays, while often complex, could be represented by relatively straightforward linear models.

As the pulsed power supplies became more compact, the systems became more complicated and more difficult to model accurately. The capacitors and inductors were replaced with synchronous machines whose functions and physical properties had to be included in the simulation.

The primary complicating factors in representing the physical system accurately were the nonlinearities present in the mutual couplings between the synchronous field, the armature, and the parasitic elements that form the electromechanical energy conversion system. In addition, the internal machine resistances vary as a function of temperature to an extent that required their effect to be included in the model.

The multi-phase power converters are modeled as simple variable resistances. The switch elements are controllable and their turn-off and turn-on are represented as resistance slopes. The detailed dynamic behavior of the switching devices is not included in the present version of the simulation in order to conserve computation time. However, a fast and accurate model for diode turn-off has been formulated and will be included in a future version of the code [14]. In addition, a simplified closed-form model of SCR turn-on is available and can be used if necessary [15].

The rail gun is represented as a set of fixed inductances and resistances and nonlinear variable impedance. The rail gun armature behavior is represented by a linear contact transition model that includes side loading and friction.

The system circuit model is shown in Fig. 3 and a detailed electrical layout is shown in Fig. 4. The method of analysis that led to the formulation follows the method outlined in [16]. The variables used in the model are defined in this figure, except as noted below. The circuit is a separately excited synchronous generator driving a simple railgun. Discharging a capacitor into the field circuit starts the self-excitation process. The branch currents are given by

$$[\dot{\mathbf{i}}] = \frac{[\mathbf{R} + \mathbf{L}'(\theta, \omega)][\mathbf{i}] + [\mathbf{v}]}{[\mathbf{L}(\theta)]} \tag{1}$$

The inductance is represented as a cosine function. Note that the machine inductances are functions of rotor position and the speed voltages are functions of angular velocity and rotor position.

The term representing the electromechanical conversion is

$$\dot{\omega} = [\mathbf{i}]\frac{1}{2J}[\mathbf{L}'(\theta, \omega)][\mathbf{i}] \tag{2}$$

where J is the rotor polar moment of inertia.

The rotor position and velocity are written as

$$\dot{\theta} = \omega \tag{3}$$

and the term representing the seed circuit is

$$\dot{V}_{sd} = \frac{i_{sd}}{C} \tag{4}$$

The loop equation for the muzzle circuit is

$$\dot{i}_{17} = \frac{V_{arm} - R_{muz}i_{17} - (x_f - x)R'i_{17} + L'vi_{17}}{L_{muz} + L'(x_f - x)} \tag{5}$$

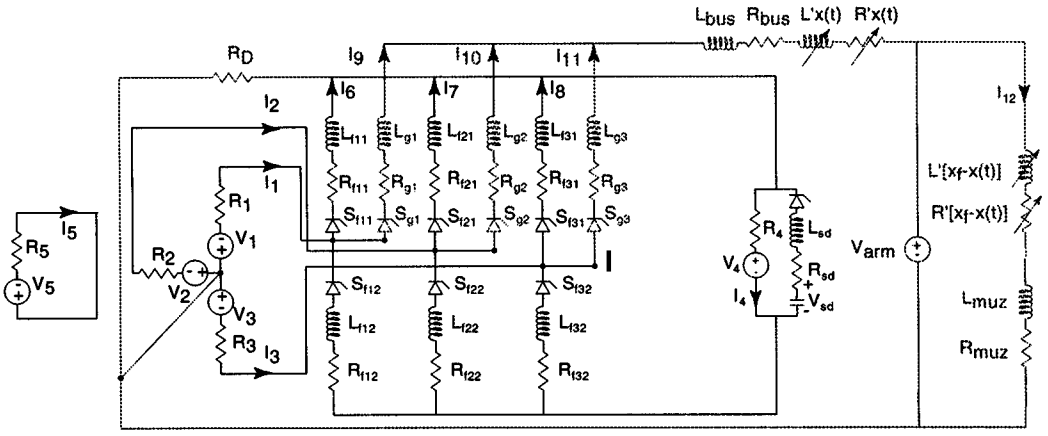

Fig. 3. Simplified circuit for the performance model.

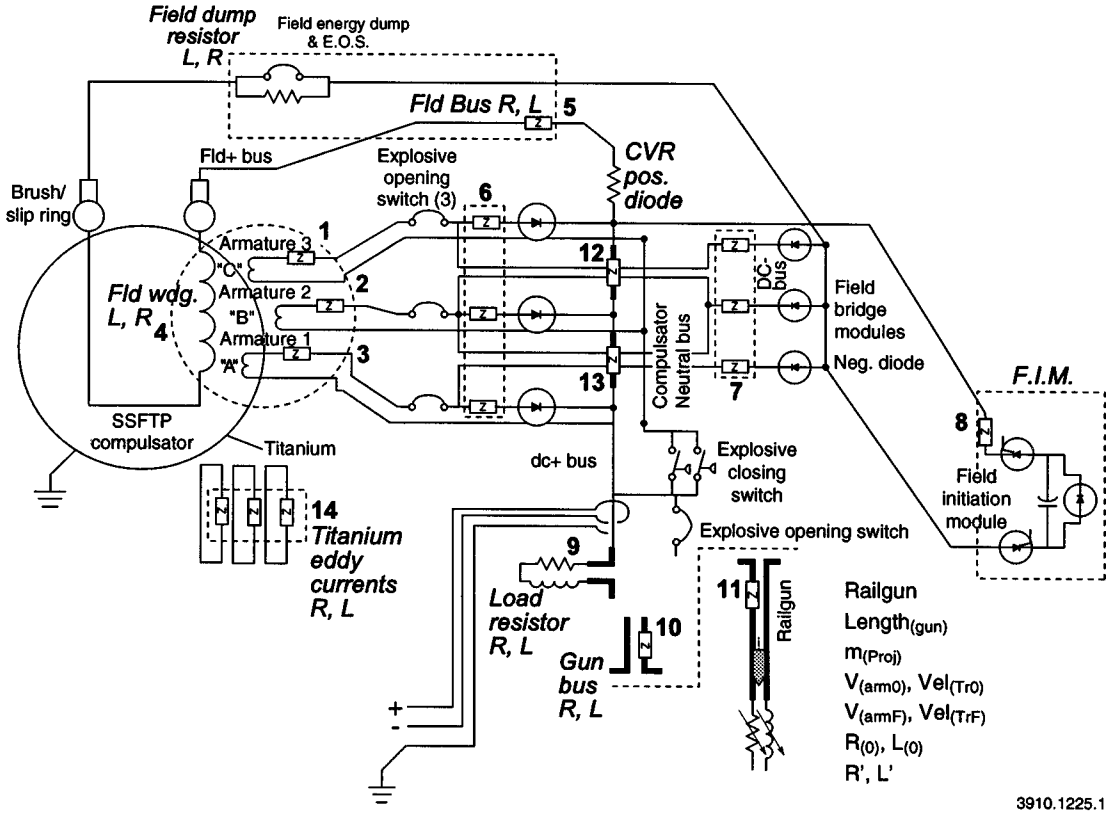

Fig. 4. Detailed pulse power schematic for scale compulsator system.

and the projectile equations of motion are

$$v = \frac{L' i_g^2 - L' i_{17}^2}{2m} \tag{6}$$

where m is the mass of the projectile, and

$$\dot{x} = v \tag{7}$$

A. Performance Comparison with Predictions

Performance results from full speed discharge sequences into a fixed resistor and cannoncaliber railgun are plotted in Figs. 5–11, and compared to results predicted from the design model in each case. The generally close alignment of result to prediction supports the value of the system-based design approach used in development of this CPA, but it is the differences that are most instructive.

B. Field Coil Current versus Time (Fig. 5)

Seed current is injected from the 50 kJ capacitors, causing the current to rise exponentially to its target value (a set time point for the system being tested), when the closing switch is actuated. The action of the closing switch is responsible for the short time difference between simulated and actual data; the timer expired just after the firing angle passed, forcing the rotor to make an additional revolution before initiating the closing switch. The armature reacted during the high current gun event, causing the AC transient recorded in the plot—a result which emphasizes

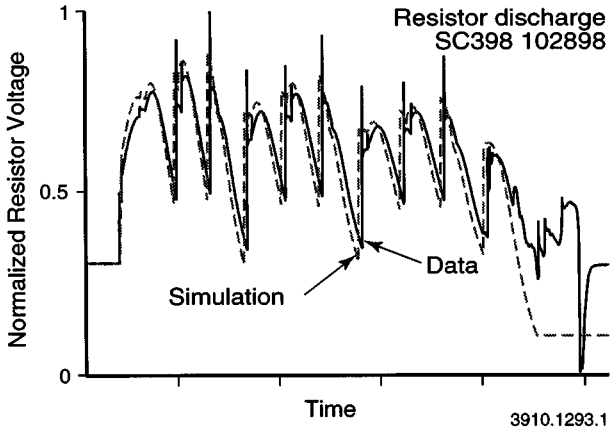

Fig. 5. Field current for two experiments and predicted results.

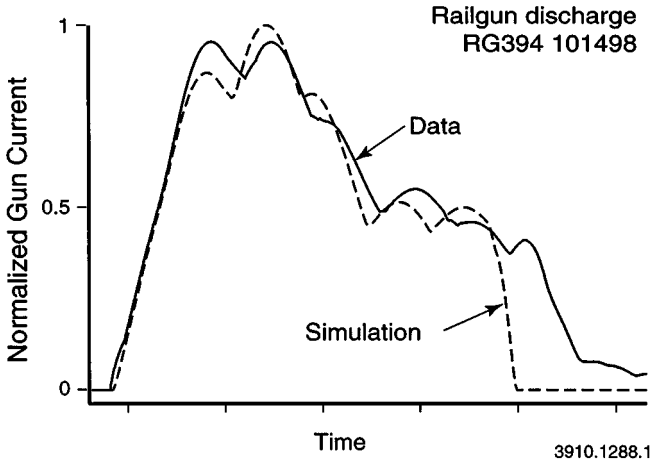

Fig. 6. Railgun current data waveform compared to predicted curve.

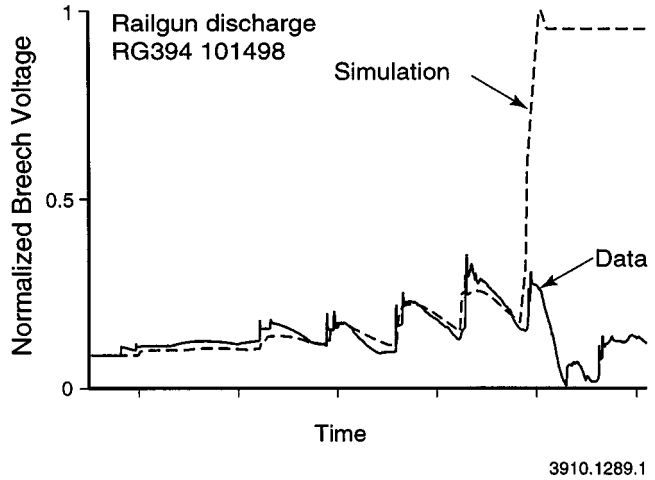

Fig. 7. Railgun breech voltage data compared with predicted curve.

the importance of including all winding interactions within the generator, in order to prevent voltage, current, and heating reactions from the armature.

C. Output Current versus Time (Fig. 6)

Experimental data varied from predictions slightly at the beginning of the current trace, and more dramatically at the end.

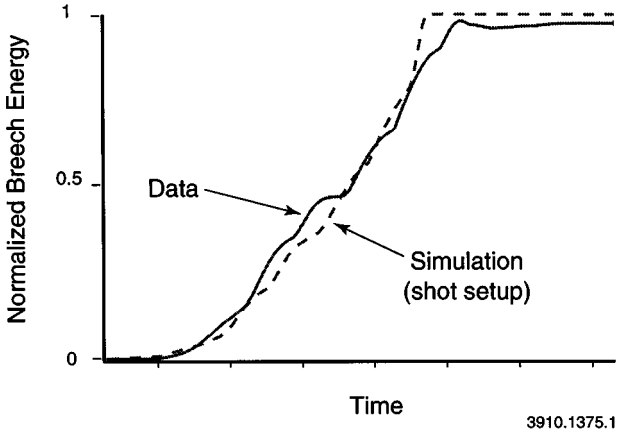

Fig. 8. Railgun breech energy data compared with prediction.

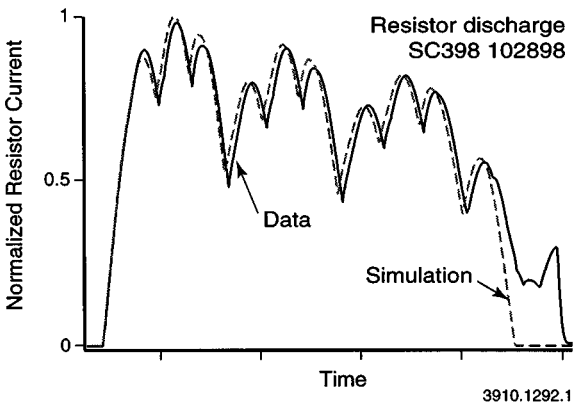

Fig. 9. Load resistor current data compared with prediction.

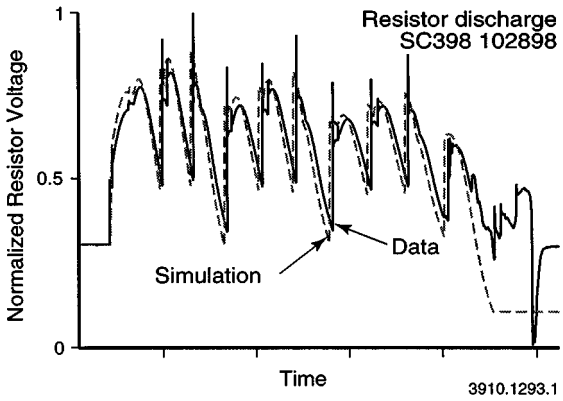

Fig. 10. Load resistor voltage data compared with predicted data.

The first anomaly results from a variance in switch performance time (180 to 280 μs), and the second from the response of the DC opening switch, which is slower than predicted.

D. Breech Voltage versus Time (Fig. 7)

The high current jump at the end of the simulation trace results from the need to pinpoint the moment the projectile exits from the railgun. The model closes the end of the launcher with a 1 kΩ resistor once the projectile is clear. This fixed resistance does not accurately portray the behavior of the muzzle arc, but it is a simple and effective way to terminate the simulation. There

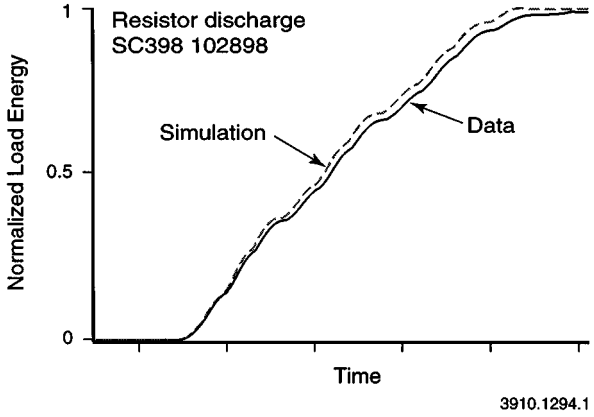

Fig. 11. Load resistor delivered energy data versus predicted data.

is no attempt in the simulation to accurately predict current flow after projectile exit.

E. Delivered Breech Energy versus Time (Fig. 8)

In this experiment, B-dot data was lost, so the precise time of projectile exit is unknown. The range of exit times shown is extrapolated from other available data, including breech voltage and rail current.

F. Railgun Simulation Test (Figs. 9–11)

This test (conducted later than the others) was designed to deliver maximum energy from the CPA into a fixed load for a time interval that simulated a railgun barrel 6 or 7 m in length. The load selected was stainless steel coax with 1.85 mΩ resistance. Inspection of the simulation and data traces shows that the CPA performance matched well with predictions.

IV. Summary

The scale CPA system discussed in this paper affirms the value of a system-wide design approach, in that performance results so closely matched simulation predictions. The system is currently operational and available for future research. Further CPA development may include replacing the diode bridge with an actively controlled SCR bridge, as well as other switch development uses for the power supply. The unit itself could be used in EMI shielding experiments, and to provide power in railgun and armature development.

Acknowledgment

The authors would like to recognize the efforts of the technical staff at UT-CEM for their hard work and attention to details. From other organizations, appreciation is extended to: R. Rodriguez and W. Crewson, Science Applbications International Corporation; E. Schmidt, Maj. M. Smith, J. Tzeng, and B. Burns, U.S. Army Research Laboratory; A. Alexander, K. Twigg, and D. Russo, Custom Analytical Engineering Systems, Inc.; J. Serjeant, State University of New York at Buffalo; I. McNab and D. Eccleshal, University of Texas Institute for Advanced Technology.

References

[1] B. M. Carder, "Driving parallel flashlamps with a compensated pulsed alternator," in *Fourteenth Pulse Power Modulator Symposium*, Orlando, FL, June 3–5, 1980.

[2] M. L. Spann *et al.*, "The design, assembly, and testing of an active rotary flux compressor," in *Third IEEE International Pulse Power Conference*, Albuquerque, NM, June 1–3, 1981.

[3] M. D. Werst, D. E. Perkins, S. B. Pratap, M. L. Spann, and R. F. Thelen, "Testing of a rapid fire, compensated pulsed alternator system," *IEEE Trans. Magn.*, vol. 25, January 1989.

[4] J. R. Kitzmiller, R. W. Faidley, R. N. Headifen, R. L. Fuller, and R. F. Thelen, "Manufacturing and testing of an air-core compulsator driven 0.60 caliber railgun system," *IEEE Trans. Magn.*, vol. 29, January 1993.

[5] A. W. Walls *et al.*, "A field based, self-excited compulsator power supply for a 9 MJ railgun demonstrator," *IEEE Trans. Magn.*, vol. 27, January 1991.

[6] J. R. Kitzmiller, S. B. Pratap, M. D. Werst, C. E. Penney, T. J. Hotz, and B. T. Murphy, "Laboratory testing of the pulse power system for the cannon caliber electromagnetic gun system (CCEMG)," *IEEE Trans. Magn.*, vol. 31, January 1995.

[7] F. J. Young *et al.*, "Interactive railgun launcher simulation," *IEEE Trans. Magn.*, vol. mag-18, 1982.

[8] D. J. Hildenbrand, "Development and validation of the ARDEC Army Railgun Modular Simulator (ARMS)," *IEEE Trans. Magn.*, vol. 29, 1993.

[9] M. Cowan, "Solid armature railguns without velocity skin effect," *IEEE Trans. Magn.*, vol. 29, 1993.

[10] J. P. Barber and A. Challita, "Velocity effects on metal armature contact transition," *IEEE Trans. Magn.*, vol. 29, 1993.

[11] J. H. Batteh *et al.*, "Effect of transient current profile on the dynamics of railgun arcs," *IEEE Trans. Magn.*, vol. 29, 1993.

[12] J. P. Barber *et al.*, "Non-arcing commutation in explosive opening switches," *IEEE Trans. Magn.*, vol. 29, 1993.

[13] T. A. Aanstoos *et al.*, "Design and fabrication of a tandem, five megampere initiate switch for the battery upgraded supply," *IEEE Trans. Magn.*, vol. 29, 1993.

[14] H. Zhang and J. A. Pappas, "A moving boundary diffusion model for PIN diodes," *IEEE Trans. Magn.*, vol. 37, 1997.

[15] W. H. Tobin, "Effect of gate configuration on thyristor plasma properties," in *IEE IAS Conference Record, IEE IAS Annual Meeting*, 1978.

[16] P. C. Krause *et al., Analysis of Electric Machinery*: IEEE Press, 1995, ch. 5, 6, 7, 10, 12.